Commensurability effect in diblock copolymer lamellar phase under d-dimensional nanoconfinement

ARTICLE *in* THE JOURNAL OF CHEMICAL PHYSICS · SEPTEMBER 2010

Impact Factor: 2.95 · DOI: 10.1063/1.3489685 · Source: PubMed

3 AUTHORS, INCLUDING:

Cheolmin Park
Yonsei University
127 PUBLICATIONS **4,188** CITATIONS
SEE PROFILE

Yong Kwon
Inha University
49 PUBLICATIONS **564** CITATIONS
SEE PROFILE

Commensurability effect in diblock copolymer lamellar phase under *d*-dimensional nanoconfinement

June Huh,[1,a)] Cheolmin Park,[1,b)] and Yong Ku Kwon[2]
[1]*Department of Materials Science and Engineering, Yonsei University, 134 Shinchon-dong, Seodaemun-gu, Seoul 120-749, Korea*
[2]*Department of Polymer Science and Engineering, Inha University, 253 Yonghyun-dong, Nam-gu, Incheon 402-751, Korea*

(Received 15 July 2010; accepted 25 August 2010; published online 16 September 2010)

We theoretically consider the commensurability problem of *AB* diblock lamellar phase confined between parallel plates, in cylinder, and in sphere calculating the free energy of confined lamellar phase which is generalized in terms of dimensionality of confinement (d) and conformational asymmetry (ϵ). We find that the first-order layer-addition transition of lamellar layers parallel to the confining surface ($L_{\parallel}$) becomes suppressed as the dimensionality of confinement increases. For lamellae confined in curved space, the conformational asymmetry alters the location of layer-addition transition point and the stability of $L_{\parallel}$ against nonconcentric layers. When the surface-preferential block becomes flexible, the radius of cylindrically or spherically confined space at the layer-addition transition, where the number of *A*-*B* layers of $L_{\parallel}$ changes from l layers to $l+1$ layers, increases if l is odd and decreases otherwise due to the tendency of less flexible block filling innermost layer. The curved space also weakens the stability $L_{\parallel}$ competing with nonconcentric layers when the surface-preferential block becomes less flexible. The phase maps in the parameter space of conformational asymmetry and degree of confinement are constructed for different cases of the confinement dimensionality and the surface fields, demonstrating the effects of various system variables on the confined lamellar structures. © *2010 American Institute of Physics*. [doi:10.1063/1.3489685]

I. INTRODUCTION

Nanoscopic confinement of ordered fluids such as liquid crystals induces many intriguing behaviors regarding order-disorder transition, orientational order, and frustration that may directly couple to the confining surface, which has drawn much interest both in the industry and academia. As a macromolecular analog of smectic liquid crystals, diblock copolymer lamellar phase, which displays distinctive layered nanostructure and ordering transition driven by incompatibility between two covalently linked polymer blocks (*A* and *B* blocks), has all the richness with respect to various confinement-induced behaviors.[1–3] A typical example is the alteration of period and orientation of lamellar diblock confined between two parallel flat plates, which relates to the commensurability of the plate separation distance D with the natural lamellar period L_b. Provided that the inner surfaces of both plates attract preferentially one of the two blocks (say *A* block), the lamellar phase parallel to the surfaces, both of which are wetted by *A* block (symmetric parallel lamellar phase), is stable if $D=nL_b$, where n is a positive integer. If $D \neq nL_b$, on the other hand, the symmetric parallel lamellar phase in either compressed or stretched state competes for stability with lamellar phase normal to the surface or antisymmetric parallel lamellar phase which must pay energetic penalty associated with the elimination of wetting interactions in compensation for saving otherwise elastic penalty associated with compression or stretching of the symmetric parallel lamellar phase. This issue has been studied theoretically for strongly segregated[4–6] and weakly segregated[7] block copolymer films. It should be pointed out that the relative stability of those one-dimensionally confined lamellar morphologies having different number of layers, symmetry, and orientation is independent on the conformational asymmetry, which is the term referred to as dissimilarity in flexibility between *A* and *B* blocks. However, when the confined geometry is nonplanar, such conformational characteristic of diblock copolymer can have a significant influence on packing of diblock lamellae into a confined volume.

Here, we theoretically consider the commensurability problem of conformationally asymmetric diblock lamellar phase confined in nanospace with curved geometries to study how the curved surface, interplaying with conformational asymmetry, affects the commensurability behavior of the confined diblock lamellar phase. Three cases of confined geometries are considered in terms of the dimensionality of confinement d. The simplest case, $d=1$, denotes the slit geometry such that diblock lamellar phase is confined in one axis and unconfined in the other two axes. The case of $d=2$ corresponds to cylindrical confinement where the space is confined circularly in two axes and unconfined in the remaining axis. Likewise, the $d=3$ represents spherical confinement where the space is closed in three axes.

Diblock lamellar phase in confined geometries other than parallel plates has been studied recently by both experi-

[a)]Electronic mail: junehuh@yonsei.ac.kr.
[b)]Electronic mail: cmpark@yonsei.ac.kr.

ments and simulations which demonstrate confined morphologies in cylindrical[8–17] or spherical pore.[18–23] These studies have identified various stable or metastable confined morphologies ranging from curvature-conforming concentric lamellae to more complex structures such as toroid and catenoid. Although the previous works are partly successful to interpret those confined morphologies correlated with the curved geometry, some critical issues remain unresolved. One basic but nevertheless unexplained phenomenon is about the layer-addition transition at which the concentric lamellae with l repeating layers (each of which consists of the A-B concentric sublayers) transforms to that with $l+1$ layers upon increasing pore diameter. A recent experimental study by Shin *et al.*[8] on the polystyrene-polybutadiene (PS-PBD) diblock lamellar phase confined in cylindrical nanopore has reported an unexpected morphological behavior that only a single layer ($l=1$) is formed even at $D/L_b \cong 1.91$ (D is pore diameter). Another similar experiment but with polystyrene-poly (methyl methacrylate) (PS-PMMA) diblock lamellar phase by Sun *et al.*[10] reported that two layers are formed at $D/L_b \cong 1.54$. Simulation results supported the latter between two contradicted experimental results, reporting that the first-order layer-addition transition from $l=1$ to $l=2$ occurs at $D/L_b \cong 1.58$.[15] Considering that those simulations were done only for conformationally symmetric block copolymer and that PS-PMMA is more conformationally symmetric than PS-PBD, it is inferred that the conformational asymmetry plays a significant role in the commensurability behavior of lamellar confined in the curved geometry. On the theoretical side, the strong stretching theory based on the curvature expansion leads to an even larger deviation from experiment and simulation results, misplacing the transition from $l=1$ to $l=2$ at $D/L_b=1.0$.[15] Besides, the predicted layer-addition transitions are second-order, in disagreement with the simulation results. The failure of the strong stretching theory both in qualitative and quantitative levels is, rather than due to the framework of strong stretching theory itself, more likely due to the curvature expansion approach,[24] where the free energy of confined lamellar in flat geometry is expanded with respect to the curvature in the lowest order. Bearing these issues in mind, we develop a theoretical model for d-dimensionally confined diblock lamellar phase in Sec. II.

II. THEORY

We consider a strongly segregated AB diblock copolymer melt filled in d-dimensionally confined space with a mean segmental density ρ_o. The A block of a diblock copolymer consists of fN segments each of which has a segment length a, and the B block consists of $(1-f)N$ segments with segment length ϵa, where the parameter ϵ represents the dissimilarity in flexibility between two blocks. Three energetic parameters are denoted by γ_{AB}, γ_{AS}, and γ_{BS}, where $\gamma_{\alpha\beta}$ is the α/β interfacial tension (the subscript S stands for the confining surface). The bulk free energy per chain of the strongly segregated lamellar F_b and the bulk lamellar period L_b have the form of $F_b=3\mathcal{S}_b^{1/3}(\mathcal{I}_b/2)^{2/3}$ and $L_b=2R_b=(4\mathcal{I}_b/\mathcal{S}_b)^{1/3}$ with $\mathcal{S}_b=\pi^2[f+(1-f)/\epsilon^2]/(8Na^2)$ and $\mathcal{I}_b=\gamma_{AB}N/\rho_o$. The confined volume of d-dimensional confinement V can be written in terms of d by $V=\pi^{d/2}R^dH^{3-d}/\Gamma(d/2+1)$, where $R(=D/2)$ is the half separation distance ($d=1$) or radius ($d=2$ or 3) of confined space, H is the transverse dimension, and $\Gamma(x)$ is the gamma function. The free energy per chain of confined lamellar in the strong segregation regime is the sum of four terms: $F=F_A+F_B+F_{AB}+F_S$, where the first two terms are the stretching energies of A and B block, and the last two terms represent the A/B interfacial energy and surface/polymer interfacial energy, respectively. The stretching energies per chain can be computed by $F_A=(F_b/R_b^2)\int_{V_A}d\mathbf{r}z^2/(\kappa f^2V)$ and $F_B=(F_b/R_b^2)\int_{V_B}d\mathbf{r}z^2/(\kappa\epsilon^2(1-f)^2V)$, where $\int_{V_\alpha}$ indicates an integral over the volume of α-domain in the confined space ($\alpha=A$ or B), z is the shortest distance from the A/B interface, and $\kappa=f+(1-f)/\epsilon^2$. The interfacial energies per chain are given as $F_{AB}=2F_bR_b\mathcal{A}_{AB}/(3V)$ and $F_S=2F_bR_b(2\tilde{\gamma}_{AS}\mathcal{A}_{AS}+\Delta\tilde{\gamma}\mathcal{A}_{BS})/(3V)$, where $\mathcal{A}_{\alpha\beta}$ is the α/β interfacial area, $\tilde{\gamma}_{\alpha S}=\gamma_{\alpha S}/\gamma_{AB}$, and $\Delta\tilde{\gamma}=\tilde{\gamma}_{BS}-\tilde{\gamma}_{AS}$. Here, the case $\Delta\tilde{\gamma}>0$, i.e., the surface attracts preferentially A block, is considered without loss of generality.

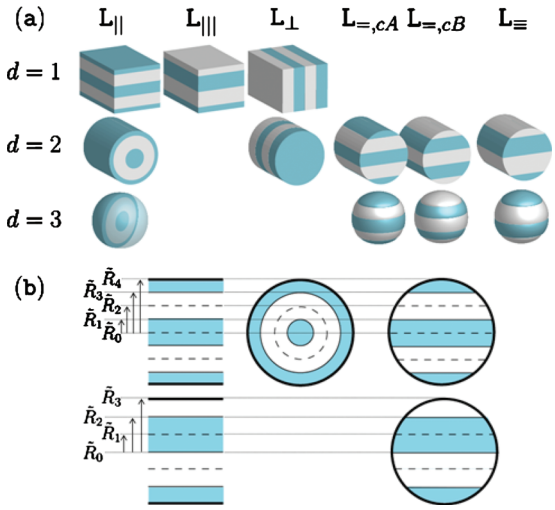

FIG. 1. (a) d-dimensionally confined lamellar morphologies for $L_{\parallel}$, $L_{|||}$, $L_{\perp}$, $L_{=,cA}$, $L_{=,cB}$, and $L_{\equiv}$. (b) The schematic representation of the geometries for $L_{\parallel}$ and $L_{=,cA}$ with $\nu=4$ (upper side) and for $L_{|||}$, and $L_{\equiv}$ with $\nu=3$ (lower side).

Confined lamellar structure can be classified into two categories in terms of the surface coverage: CW (complete wetting) structures where A block coats completely the surface and PW (partial wetting) structures where A and B blocks share the surface coverage with certain wetting geometries. While there are a number of possible structures for CW and PW structures, here we restrict our consideration to the following basic structures: symmetric lamellae parallel to the surface ($L_{\parallel}$) for CW structures, asymmetric lamellae parallel to the surface ($L_{|||}$), lamellae stacked in the unconfined direction ($L_{\perp}$), symmetric and asymmetric lamellae stacked in one of confined directions ($L_{=}$, $L_{\equiv}$) for PW structures [see Fig. 1(a)].

We first consider symmetric lamellar phase parallel to the surface $L_{\parallel}$. For describing multilayers, it is necessary to introduce a positive integer ν defined as the number of A/B

interface points counted along the diameter in the radial cross-section of confined volume [see Fig. 1(b)]. For $L_{\parallel}$, ν is even numbers and relates to the number of layers l (or the number of A/B interfaces): $l=\nu$ if $d=1$ and $l=\nu/2$ otherwise. In what follows, we express all the free energies and the length scales in unit of the bulk free energy F_b and the half bulk period R_b such that $\tilde{F}=F/F_b$ and $\tilde{R}=R/R_b$. By the consideration of geometry for $L_{\parallel}$, the contributions to the normalized free energy per chain for $L_{\parallel}$ with ν ($\tilde{F}_{\parallel,\nu}=\tilde{F}_{\parallel,\nu,A}+\tilde{F}_{\parallel,\nu,B}+\tilde{F}_{\parallel,\nu,AB}+\tilde{F}_{\parallel,S}$) can be formulated in terms of d. The results are

$$\tilde{F}_{\parallel,\nu,A}=\frac{1}{f^2\kappa V R_b^2}\int_{V_A} d\mathbf{r}z^2=\frac{1}{f^2\kappa\tilde{R}^d}\left[\frac{1-(-1)^{\nu/2}}{2}\left\{\frac{d}{d+2}\left(\tilde{R}_2^{d+2}+\sum_{i=1}^{(\nu-2)/4}(\tilde{R}_{4i+2}^{d+2}-\tilde{R}_{4i-2}^{d+2})\right)-\frac{2}{(d+1)(d+2)}\right.\right.$$
$$\times\left(\tilde{R}_1^{d+2}-\sum_{i=1}^{(\nu-2)/4}(\tilde{R}_{4i-1}^{d+2}-\tilde{R}_{4i+1}^{d+2})\right)-\frac{2d}{d+1}\left(\tilde{R}_1\tilde{R}_2^{d+1}+\sum_{i=1}^{(\nu-2)/4}(\tilde{R}_{4i+1}\tilde{R}_{4i+2}^{d+1}-\tilde{R}_{4i-1}\tilde{R}_{4i-2}^{d+1})\right)+\tilde{R}_1^2\tilde{R}_2^d$$
$$\left.+\sum_{i=1}^{(\nu-2)/4}(\tilde{R}_{4i+1}^2\tilde{R}_{4i+2}^d-\tilde{R}_{4i-1}^2\tilde{R}_{4i-2}^d)\right\}+\frac{1+(-1)^{\nu/2}}{2}\left\{\frac{d}{d+2}\sum_{i=0}^{(\nu-4)/4}(\tilde{R}_{4i+4}^{d+2}-\tilde{R}_{4i}^{d+2})+\frac{2}{(d+1)(d+2)}\sum_{i=0}^{(\nu-4)/4}(\tilde{R}_{4i+1}^{d+2}-\tilde{R}_{4i+3}^{d+2})\right.$$
$$\left.\left.-\frac{2d}{d+1}\sum_{i=0}^{(\nu-4)/4}(\tilde{R}_{4i+3}\tilde{R}_{4i+4}^{d+1}-\tilde{R}_{4i+1}\tilde{R}_{4i}^{d+1})+\sum_{i=0}^{(\nu-4)/4}(\tilde{R}_{4i+3}^2\tilde{R}_{4i+4}^d-\tilde{R}_{4i+1}^2\tilde{R}_{4i}^d)\right\}\right], \tag{1}$$

$$\tilde{F}_{\parallel,\nu,B}=\frac{1}{(1-f)^2\epsilon^2\kappa V R_b^2}\int_{V_B} d\mathbf{r}z^2=\frac{1}{(1-f)^2\epsilon^2\kappa\tilde{R}^d}\left[\frac{1-(-1)^{\nu/2}}{2}\left\{\frac{2}{(d+1)(d+2)}\left(\tilde{R}_1^{d+2}+\sum_{i=1}^{(\nu-2)/4}(\tilde{R}_{4i+1}^{d+2}-\tilde{R}_{4i-1}^{d+2})\right)\right.\right.$$
$$\left.+\frac{2d}{d+1}\sum_{i=1}^{(\nu-2)/4}\tilde{R}_{4i}^{d+1}(\tilde{R}_{4i+1}-\tilde{R}_{4i-1})-\sum_{i=1}^{(\nu-2)/4}\tilde{R}_{4i}^d(\tilde{R}_{4i+1}^2-\tilde{R}_{4i-1}^2)\right\}+\frac{1+(-1)^{\nu/2}}{2}\left\{\frac{2}{(d+1)(d+2)}\sum_{i=0}^{(\nu-4)/4}(\tilde{R}_{4i+3}^{d+2}-\tilde{R}_{4i+1}^{d+2})\right.$$
$$\left.\left.+\frac{2d}{d+1}\sum_{i=0}^{(\nu-4)/4}\tilde{R}_{4i+2}^{d+1}(\tilde{R}_{4i+3}-\tilde{R}_{4i+1})-\sum_{i=0}^{(\nu-4)/4}\tilde{R}_{4i+2}^d(\tilde{R}_{4i+3}^2-\tilde{R}_{4i+1}^2)\right\}\right], \tag{2}$$

$$\tilde{F}_{\parallel,\nu,AB}=\frac{2d}{3\tilde{R}^d}\sum_{i=0}^{(\nu-2)/2}\tilde{R}_{2i+1}^{d-1}, \tag{3}$$

$$\tilde{F}_{\parallel,S}=\frac{2d\tilde{\gamma}_{AS}}{3\tilde{R}}, \tag{4}$$

with the constraints for conserving diblock composition f,

$$\tilde{R}_{2m+1}^d-\tilde{R}_{2m}^d=\tfrac{1}{2}[1-(-1)^{m+\nu/2}(1-2f)]\times(\tilde{R}_{2m+2}^d-\tilde{R}_{2m}^d). \tag{5}$$

Here, $\tilde{R}_m$ is the normalized radial position of A/B interface (odd m) or midplane of bilayer (even m) between origin at $\tilde{R}_o=0$ and the boundary of confined volume at $\tilde{R}_\nu=\tilde{R}$ [see Fig. 1(b)]. Noting that the normalized free energy per chain has $(\nu-2)/2$ independent radial positions due to the constraint Eq. (5), the total free energy $\tilde{F}_{\parallel,\nu}$ is minimized with respect to $\tilde{R}_{2m}$ ($1\le m\le(\nu-2)/2$) and ν, which gives $\tilde{F}_{\parallel}$ as a function of the set of parameters $(d,f,\epsilon,\tilde{\gamma}_{AS},\tilde{R})$.

We next formulate the free energies of PW structures ($L_{|||}$, $L_{\perp}$, $L_{=}$, and $L_{\equiv}$) which are competitive for stability with $L_{\parallel}$ when the surface is weakly selective. Some cases of PW structures are identical or impossible depending on the dimensionality of confinement. One can notice that the confined layers $L_{|||}$ and $L_{\equiv}$ are identical for $d=1$ and the unconfined layers (perpendicular lamellar) $L_{\perp}$ are not possible for $d=3$. The free energies of $L_{|||}$ ($\tilde{F}_{|||}$) and $L_{\perp}$ ($\tilde{F}_{\perp}$) are straightforward to formulate. Since $L_{|||}$ structure is only possible for $d=1$, we have

$$\tilde{F}_{|||\nu}=\frac{1}{3}\left[\left(\frac{2\tilde{R}}{\nu}\right)^2+\frac{1}{\tilde{R}}(\nu+2\tilde{\gamma}_{AS}+\Delta\tilde{\gamma})\right], \tag{6}$$

where ν is an odd number. The free energy of $L_{\perp}$ ($\tilde{F}_{\perp}$) that is possible for $d<3$ is given as

$$\tilde{F}_{\perp}=1+\frac{2d}{3\tilde{R}}[\tilde{\gamma}_{AS}+\Delta\tilde{\gamma}(1-f)]. \tag{7}$$

For the free energies of $L_{=}$ and $L_{\equiv}$ ($d>1$), we use a "kinked-path" *ansatz* developed by Olmsted and Milner.[25] In this treatment, the volume of a unit layer (consisting of A and B sublayers) is divided into infinitesimal A and B wedges that each satisfies the local volume constraint. Figure 2 illustrates the wedge construction for the $L_{=}$ structure which consists of two capping pieces (cap) and $2\nu-2$ sliced pieces

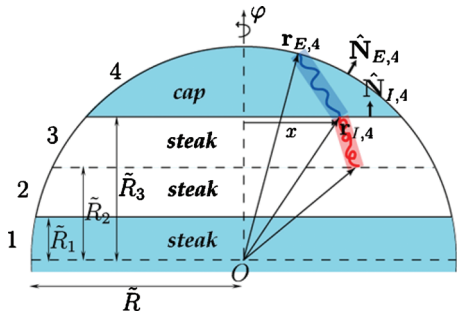

FIG. 2. The schematic of infinitesimal wedge in the $L_{=,cA}$ structure consisting of cap and steak layers for $d=3$ (see details in the Appendix).

(steak). Each of caps and steaks is divided into infinitesimal wedges. Due to the local volume conservation in the wedge for $L_{=}$, the mean trajectory, along which the block copolymer chain extends, has a kink at the A/B interface. Using the kinked path ansatz, we have the stretching energies for $L_{=}$ with A caps ($L_{=,cA}$),

$$\tilde{F}_{=,\nu,A} = \frac{\Gamma(d/2+1)}{\pi^{d/2} f^2 \kappa}\left[(1-(-1)^{\nu/2})\left(\sum_{i=0}^{(\nu-2)/4}\xi_{4i+2} + \sum_{i=0}^{(\nu-6)/4}\xi_{4i+3}\right) + (1+(-1)^{\nu/2})\sum_{i=0}^{(\nu-4)/4}(\xi_{4i+1}+\xi_{4i+4})\right], \tag{8}$$

$$\tilde{F}_{=,\nu,B} = \frac{\Gamma(d/2+1)}{\pi^{d/2}(1-f)^2 \epsilon^2 \kappa}\left[(1-(-1)^{\nu/2}) \times\left(\sum_{i=0}^{(\nu-2)/4}\xi_{4i+1} + \sum_{i=0}^{(\nu-6)/4}\xi_{4i+4}\right) + (1+(-1)^{\nu/2})\sum_{i=0}^{(\nu-4)/4}(\xi_{4i+2}+\xi_{4i+3})\right], \tag{9}$$

where ν should be even numbers and the function ξ_j for each case of $d=2$ and $d=3$ is given in the Appendix. The interfacial energies for $d=2$ are

$$\tilde{F}_{=,\nu,AB} = \frac{8}{3\pi\tilde{R}}\left[\sum_{i=1}^{\nu/2}\left(1-\frac{\tilde{R}_{2i-1}^2}{\tilde{R}^2}\right)^{1/2}\right], \tag{10}$$

$$\tilde{F}_{=,\nu,S} = \frac{2}{3\tilde{R}}\left[2\tilde{\gamma}_{AS} + \Delta\tilde{\gamma}\left(1-(-1)^{\nu/2} - \frac{4}{\pi}\sum_{i=1}^{\nu/2}(-1)^{i+\nu/2}\arccos\left(\frac{\tilde{R}_{2i-1}}{\tilde{R}}\right)\right)\right], \tag{11}$$

and those for $d=3$ are given as

$$\tilde{F}_{=,\nu,AB} = \frac{1}{\tilde{R}}\left[\frac{\nu}{2} - \sum_{i=1}^{\nu/2}\frac{\tilde{R}_{2i-1}^2}{\tilde{R}^2}\right], \tag{12}$$

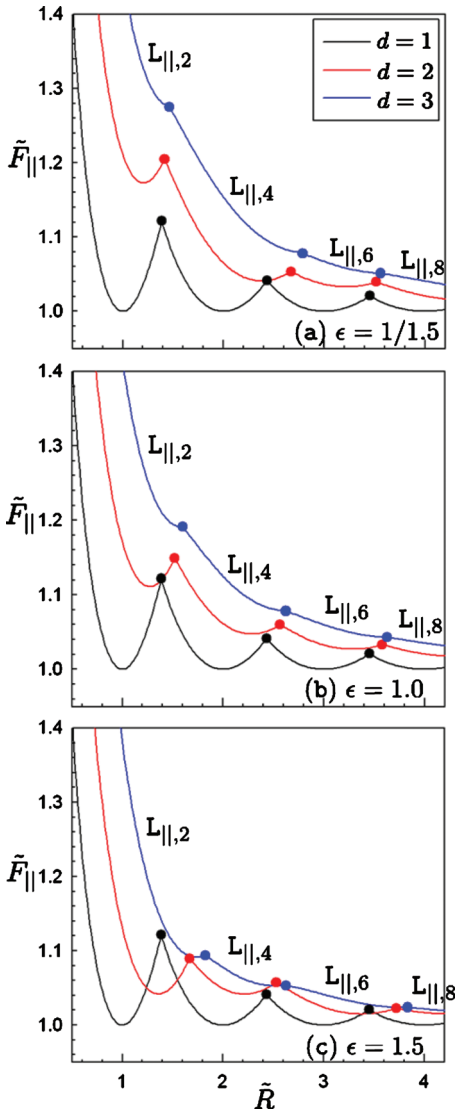

FIG. 3. The normalized free energy per chain for $L_{\parallel}$ with $\tilde{\gamma}_{AS}=0$ as a function of the normalized radius of confined space. (a) $\epsilon=1/1.5$, (b) $\epsilon=1.0$, and (c) $\epsilon=1.5$.

$$\tilde{F}_{=,\nu,S} = \frac{2}{3\tilde{R}}\left[\tilde{\gamma}_{AS} + \Delta\tilde{\gamma}\sum_{i=1}^{\nu/2}\frac{(-1)^{i+\nu/2}\tilde{R}_{2i-1}}{\tilde{R}}\right]. \tag{13}$$

The total free energy is then minimized with respect to $\tilde{R}_{2i}$ (i.e., the positions of midplane) under the constraint of composition conservation. To obtain the free energy for $L_{=}$ with B caps ($L_{=,cB}$), one should change f, $\tilde{\gamma}_{AS}$, and $\tilde{\gamma}_{BS}$ to $(1-f)\epsilon$, $\tilde{\gamma}_{BS}$, and $\tilde{\gamma}_{AS}$, respectively, in Eqs. (8), (9), (11), and (13). Similarly, the free energy of $L_{\equiv}$ can also be formulated using the kinked-path ansatz.

III. RESULTS AND DISCUSSIONS

We begin with discussing the commensurability behavior of $L_{\parallel}$ structure that is stable to PW structures if $\tilde{\gamma}_{BS} \gg \tilde{\gamma}_{AS}$. Typical results of $\tilde{F}_{\parallel}$ are plotted as a function of the radius of d-dimensionally confined volume $\tilde{R}$, as shown in Figs. 3(a)–3(c). The free energy curves show the first-order layer-addition transitions from ν to $\nu+2$ at each of cusp

points ($\tilde{R}_{\nu\to\nu+2}$, $\tilde{F}_{\|,\nu\to\nu+2}$) showing some notable trends arising from the dimensionality of confinement d and the conformational asymmetry ϵ. First, the first-order layer-addition transitions, which are distinctive for $d=1$, become suppressed for higher d. For perfectly symmetric diblock ($f=0.5$, $\epsilon=1$), the magnitude of discontinuity, which can be computed from the difference in the first derivative at the transition point, $\Delta\mathcal{F}=\partial_{\tilde{R}}\tilde{F}_{\|,\nu}(\tilde{R}_{\nu\to\nu+2})-\partial_{\tilde{R}}\tilde{F}_{\|,\nu+2}(\tilde{R}_{\nu\to\nu+2})$, is found to scale as $\Delta\mathcal{F}\sim\tilde{R}^{-2}$ for $d=1$, $\Delta\mathcal{F}\sim\tilde{R}^{-2.2}$ for $d=2$, and $\Delta\mathcal{F}\sim\tilde{R}^{-4.7}$ for $d=3$, indicating weaker first-order transition in higher dimensional case. Second, while the transition radius $\tilde{R}_{\nu\to\nu+2}$ is independent of ϵ for $d=1$, the transition radius for $d>1$ with $\epsilon<1$ [Fig. 3(a)] is shifted to a lower value if $\nu/2$ is odd and to a larger value if $\nu/2$ is even when compared to the case of $\epsilon=1$ [Fig. 3(b)] and the trend becomes opposite for $\epsilon>1$ [Fig. 3(c)]. For instance, we find for the case of $d=3$ that $\tilde{R}_{2\to4}=1.47$, $\tilde{R}_{4\to6}=2.79$ for $\epsilon=1/1.5$, and $\tilde{R}_{2\to4}=1.83$, $\tilde{R}_{4\to6}=2.63$ for $\epsilon=1.5$, indicating that the $L_{\|,\nu}$ structures with odd $\nu/2$ become more stable against that with even $\nu/2$ as ϵ increases. Because the innermost layer is B domain if $\nu/2$ is odd and A domain otherwise, this implies that when $d>1$ the stability of concentric layer having a B innermost layer becomes enhanced as ϵ increases and the other way around for the concentric layer having an A innermost layer. This behavior is understood by the following: due to the volume conservation, the layer exterior to the curved A/B interface is thinner than the layer interior to the interface for $d>1$, and therefore, the distance for chain to stretch away for packing is larger in the interior region. Since the stretching of more flexible polymer block costs larger stretching energy, less flexible block has a propensity to fill the interior region of the curved A/B interface.

The results shown in Fig. 3 suggest that the aforementioned experimental inconsistency between PS-PBD and PS-PMMA block copolymers about $\tilde{R}_{\nu=2\to\nu=4}$ in cylindrically confined space may be germane with the difference in conformational asymmetry between the two systems. Using the molecular parameters for those experimental systems ($f=0.53$, $\epsilon=1.88$ for PS-PBD and $f=0.5$, $\epsilon=1.05$ for PS-PMMA),[26] the theory predicts that $\tilde{R}_{\nu=2\to\nu=4}\cong1.76$ for PS-PBD and $\tilde{R}_{\nu=2\to\nu=4}\cong1.53$ for PS-PMMA, which qualitatively explains the reason why $\tilde{R}_{\nu=2\to\nu=4}$ for PS-PBD should be larger than that for PS-PMMA although the theoretical prediction of $\tilde{R}_{\nu=2\to\nu=4}$ for PS-PBD is still lower than the experimental value ($\tilde{R}_{\nu=2\to\nu=4}>1.9$). This quantitative disagreement between theory and the experiment for PS-PBD is possibly due to errors in molecular parameters or imperfect cylindrical geometry in the experiment and due to the strong segregation limit used in the theoretical formulation.

When the surface is weakly selective for A block, the PW structures are competitive with $L_{\|}$ structure. In Fig. 4, the phase maps for d-dimensionally confined block copolymer with $f=0.5$ are constructed in the ϵ-$\tilde{R}$ plane, where three cases of interfacial tension differences, $\Delta\tilde{\gamma}=0.1, 0.2$, and 0.3 with a fixed value of $\tilde{\gamma}_{AS}=0.0$, are considered. For the simplest case, $d=1$ (top row in Fig. 4), the phase boundaries are independent of ϵ and the regions of $L_{\perp}$ are enlarged only vertically in the phase maps as $\Delta\tilde{\gamma}$ decreases. The phase maps for $d>1$ (middle and bottom rows in Fig. 4) show more complex behaviors about the stability of PW structures. One main feature in this nonplanar confinement case is that PW structures are more stable in the region of $\epsilon<1$ where the surface-preferential A-block is less flexible than B- block. In the case of $d=2$, $L_{\perp}$ or $L_{\equiv,\nu=1}$ is stable only in the limited region of $\epsilon<1$ and $\tilde{R}<1.8$ when $\Delta\tilde{\gamma}=0.3$ [see Fig. 4(f)]. When the surface becomes less selective, the region of $L_{\perp}$ is expanded diagonally in the phase map, which indicates that not only the commensurability of R_b with R but also the conformational asymmetry significantly affects the relative stability of $L_{\|}$ and $L_{\perp}$ structures. It is also found for $d=2$ that $L_{=,\nu}$ and $L_{\equiv,\nu>1}$ are unstable to $L_{\perp}$ or $L_{\|}$. Only $L_{\equiv,\nu=1}$ is stable for small values of ϵ when the surface is moderately or strongly selective [Figs. 4(e) and 4(f)]. Similar but more complicated changes in phase boundaries are found for the case of $d=3$. The stacked layer structures, $L_{=}$ or $L_{\equiv}$, become stable to the concentric layer structure ($L_{\|}$) as both ϵ and $\Delta\tilde{\gamma}$ decrease. Since more flexible block has an entropy-originated propensity to form the outermost layer of the $L_{\|}$ structure, the $L_{\|}$ structure dominates in the region of large ϵ where the spherical surface favors A block not only energetically but also entropically. The $L_{\|}$ structure becomes unstable if the surface-preferential block becomes less flexible and is replaced by $L_{=}$ or $L_{\equiv}$. Also of interest is that when the surface selectivity is weak, the layer configuration of $L_{=,2,cA}$ having a layer sequence of A-B-B-A from top cap layer to the other cap is inverted to that of $L_{=,2,cB}$ (i.e., B-A-A-B) as ϵ increases, as seen in Fig. 4(g). While the A-B-B-A configuration is energetically favored due to the larger surface area of cap layer than that of steak layer for $L_{=}$ structure, there is also an entropy-originated propensity to fill in the cap layer with less flexible block. The latter is due to the larger average and variance in distance for chain stretching in the cap layer than in the steak layer due to the volume conservation. Therefore, when ϵ is large enough such that the entropic propensity for B block forming cap layers outweighs the energetic preference for A block filling the caps, B-capped $L_{=}$ structure is favored over A-capped structure. Figure 5 presents the free energy curves of various layered structures for $\Delta\tilde{\gamma}=0.1$ and $\epsilon=1.4$ demonstrating the situation of layer inversion from $L_{=,2,cA}$ to $L_{=,2,cB}$. This layer inversion exemplifies an entropy-type interaction caused by interplay between conformational asymmetry and nonplanar surface.

IV. SUMMARY AND REMARKS

We have examined the commensurability problem of some basic layered structures formed by diblock lamellar phase confined between parallel plates ($d=1$), in cylinder ($d=2$), and in sphere ($d=3$), and their thermodynamic stability calculating the free energy of confined lamellar structure generalized in terms of the dimensionality of confinement and conformational asymmetry. We find that the first-order layer-addition transition of $L_{\|}$ structure, where the number of A-B layers changes, becomes suppressed as the dimensionality of confinement increases. For diblock lamellar phase

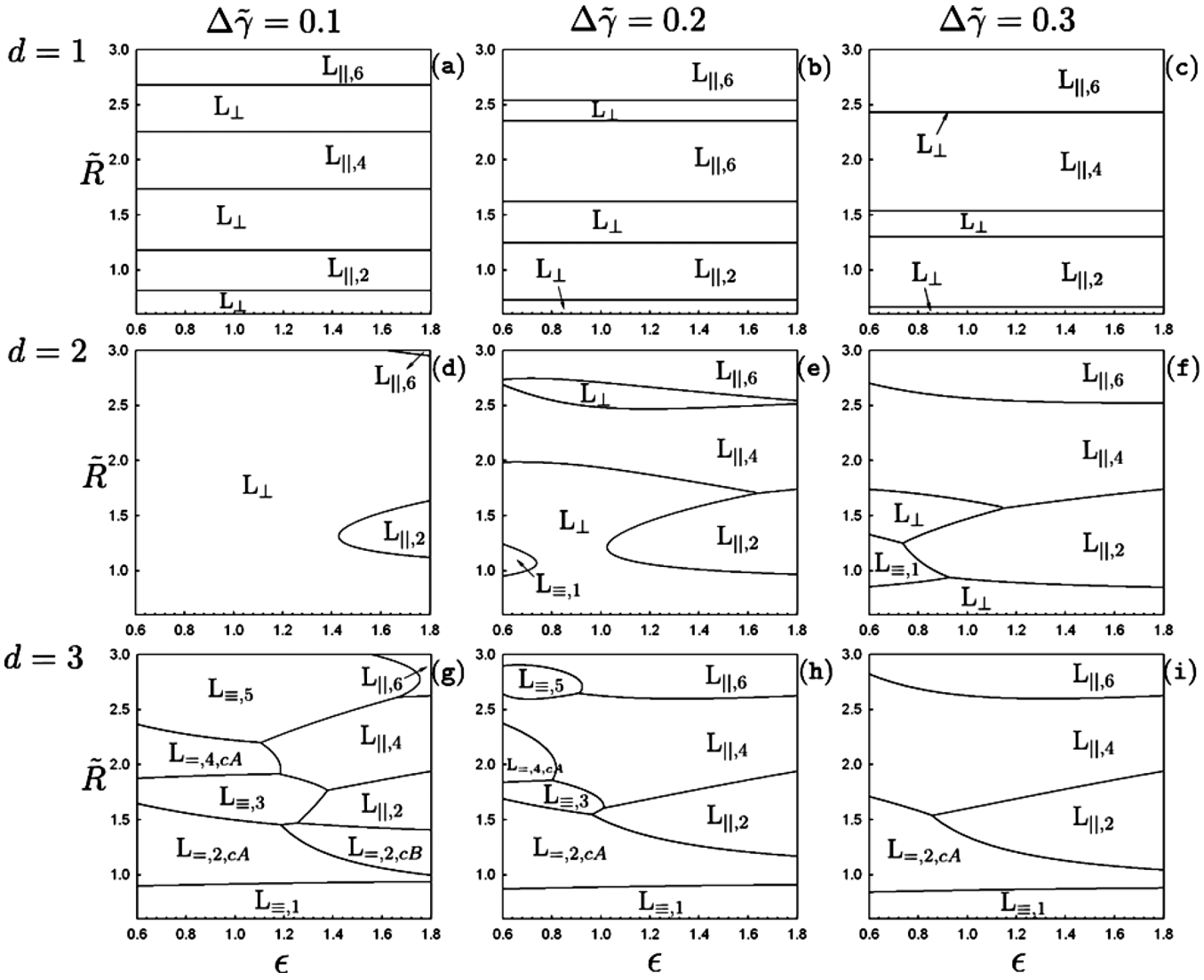

FIG. 4. The phase maps of d-dimensionally confined lamellar constructed in the ϵ-$\tilde{R}$ plane for $f=0.5$ and $\gamma_{AS}=0.0$. The phase maps in different columns represent the different cases of $\Delta\tilde{\gamma}$ and those in different rows represent the different cases of the confinement dimensionality.

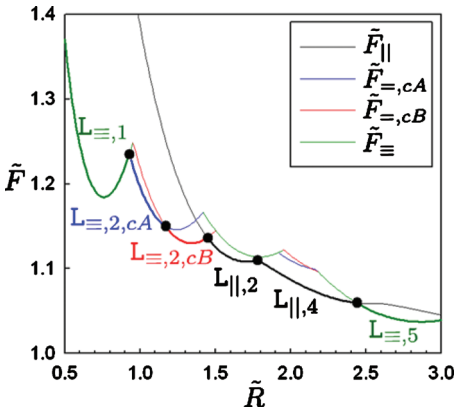

FIG. 5. The normalized free energy per chain of $L_{||}$, $L_{=,cA}$, $L_{=,cB}$, and $L_{\equiv}$ as a function of the normalized radius of confined space for $d=3$, $\Delta\tilde{\gamma}=0.1$, and $\epsilon=1.4$ with $\tilde{\gamma}_{AS}=0$. The lowest free energy is represented by the thick line, and the transition points between stable structures are shown by the filled circles.

confined in curved space ($d>1$), the conformational asymmetry turns out to be an important parameter significantly affecting the location of layer-addition transition point ($\tilde{R}_{l\to l+1}$) and the stability of concentric layers. When the surface-preferential block becomes flexible, transition point $\tilde{R}_{l\to l+1}$ increases if l is odd and decreases otherwise due to the tendency of less flexible block filling innermost layer. The curved space also weakens the stability of $L_{||}$ competing with PW structures when the surface-preferential block becomes less flexible, which results in domination of PW structures in the region of $\epsilon<1$ of the $\epsilon-\tilde{R}$ phase map.

The present study considers only basic layered structures and excludes some other exotic PW structures having complicated wetting and internal geometries that might be stable in partial region of ϵ-$\tilde{R}$ space. For instance, it has been recently reported from a computational study[17] on the conformationally symmetric block copolymer under cylindrical confinement that catenoid cylinder, where the outermost

layer formed by surface preferential block is perforated by the domain formed by the other block, is identified as a stable structure when the degree of confinement is very strong ($\tilde{R}<0.8$) while the investigated parameter space is dominated by simple layered structures ($L_{\parallel}$ and $L_{\perp}$). Such exotic structures are largely due to the structural deformability which seem to be invalid in the strong segregation limit.

ACKNOWLEDGMENTS

This work was supported by the Korea Science and Engineering Foundation (KOSEF) grant funded by the Korea government (MEST) under Grant No. 2009-0083869.

APPENDIX: STRETCHING ENERGIES FOR CAP AND STEAK LAYER

Here, we formulate the function ξ_i appearing in Eqs. (8) and (9). As shown in Fig. 2, $L_{=,\nu,cA}$ structure consists of two cap A-layers, $(\nu-2)$ steak A-layers, and ν B-layers. The stacked layers are numbered in the order from the central steak layer $(i=1)$ to the cap layer $(i=\nu)$. Each layer has an A/B interface $(\mathbf{r}_{I,i})$ and the noninterfacial surface $(\mathbf{r}_{E,i})$ bound to the boundary of confinement or the midplane and the boundary of confinement where $\mathbf{r}_{I,i}$ and $\mathbf{r}_{E,i}$ describe the positions of A/B interface and the noninterfacial surface of the layer i, respectively. For $d=3$, we parametrize the interface and the noninterfacial surface by $\mathbf{r}_{I,i}(x,\varphi)$ and $\mathbf{r}_{E,i}(g_i(x),\varphi)$, where x is the lateral position on the interface, φ is the revolution angle (see Fig. 2), and the mapping $g_i(x)$ describes the lateral position on the boundary surface of the layer i. Similarly, we parametrize them for $d=2$ by $\mathbf{r}_{I,i}=\mathbf{r}_{I,i}(x)$ and $\mathbf{r}_{E,i}=\mathbf{r}_{E,i}(g_i(x))$. The mapping $g_i(x)$ should satisfy the composition constraint associated with $g_j(x)$ of the neighboring layer j where $j=2\lfloor i+1/2\rfloor-1+(-1)^i$ ($\lfloor X\rfloor$ is the floor function of X).

The wedge element is constructed by the chain path extending from $\mathbf{r}_{I,i}$ to $\mathbf{r}_{E,i}$ in terms of infinitesimal element dx and $d\varphi$. The function ξ_i, which is proportional to the stretching energy of the layer i [Eqs. (8) and (9)], is then given from the integration over wedge elements. For $d=3$, we get

$$\xi_i=\int_0^{2\pi}d\varphi\int_0^{(\tilde{R}^2-\tilde{R}_{I,i}^2)^{1/2}}dx\Psi_i(x,\varphi) \tag{A1}$$

with

$$\Psi_i=\frac{|\mathbf{r}_{IE,i}|^3}{60}\left[\hat{\mathbf{e}}_{IE,i}\cdot\hat{\mathbf{N}}_{I,i}\left|\frac{\partial\mathbf{r}_{I,i}}{\partial x}\right|\left(2\hat{\mathbf{e}}_{IE,i}\cdot\hat{\mathbf{N}}_{I,i}\left|\frac{\partial\mathbf{r}_{I,i}}{\partial\varphi}\right|+3\hat{\mathbf{e}}_{IE,i}\cdot\hat{\mathbf{N}}_{E,i}\left|\frac{\partial\mathbf{r}_{E,i}}{\partial\varphi}\right|\right)+3\hat{\mathbf{e}}_{IE,i}\cdot\hat{\mathbf{N}}_{I,i}\left|\frac{\partial\mathbf{r}_{E,i}}{\partial x}\right|\times\left(\hat{\mathbf{e}}_{IE,i}\cdot\hat{\mathbf{N}}_{I,i}\left|\frac{\partial\mathbf{r}_{I,i}}{\partial\varphi}\right|+4\hat{\mathbf{e}}_{IE,i}\cdot\hat{\mathbf{N}}_{E,i}\left|\frac{\partial\mathbf{r}_{E,i}}{\partial\varphi}\right|\right)\right], \tag{A2}$$

where $\hat{\mathbf{e}}_{IE,i}$ is the unit vector in the direction of $\mathbf{r}_{IE,i}=\mathbf{r}_{E,i}-\mathbf{r}_{I,i}$, $\hat{\mathbf{N}}_{I,i}$ and $\hat{\mathbf{N}}_{E,i}$ are the unit vectors normal to the interface and the noninterfacial surface of the layer i, respectively. For $d=2$, we have

$$\xi_i=\int_0^{(\tilde{R}^2-\tilde{R}_{I,i}^2)^{1/2}}dx\Psi_i(x) \tag{A3}$$

with

$$\Psi_i=\frac{|\mathbf{r}_{IE,i}|^3}{12}\left[\hat{\mathbf{e}}_{IE,i}\cdot\hat{\mathbf{N}}_{I,i}\left|\frac{\partial\mathbf{r}_{I,i}}{\partial x}\right|+3\hat{\mathbf{e}}_{IE,i}\cdot\hat{\mathbf{N}}_{E,i}\left|\frac{\partial\mathbf{r}_{E,i}}{\partial x}\right|\right]. \tag{A4}$$

[1] T. P. Russell, A. Menelle, S. H. Anastasiadis, S. K. Satija, and C. F. Majkrzak, Macromolecules **24**, 6263 (1991).
[2] P. Mansky, T. P. Russell, C. J. Hawker, J. Mays, D. C. Cook, and S. K. Satija, Phys. Rev. Lett. **79**, 237 (1997).
[3] C. Shin, D. Y. Ryu, J. Huh, J. H. Kim, and K.-W. Kim, Macromolecules **42**, 2157 (2009).
[4] M. S. Turner, Phys. Rev. Lett. **69**, 1788 (1992).
[5] D. G. Walton, G. J. Kellog, A. M. Mayes, P. Lambooy, and T. P. Russell, Macromolecules **27**, 6225 (1994).
[6] M. W. Matsen, J. Chem. Phys. **106**, 7781 (1997).
[7] H. J. Angerman, A. Johner, and A. N. Semenov, Macromolecules **39**, 6210 (2006).
[8] K. Shin, H. Xiang, S. I. Moon, T. Kim, T. J. McCarthy, and T. P. Russell, Science **306**, 76 (2004).
[9] H. Xiang, K. Shin, T. Kim, S. I. Moon, T. J. McCarthy, and T. P. Russell, Macromolecules **37**, 5660 (2004).
[10] Y. Sun, M. Steinhart, D. Zschech, R. Adhikari, G. H. Michler, and U. Gösele, Macromol. Rapid Commun. **26**, 369 (2005).
[11] X. He, M. Song, H. Liang, and C. Pan, J. Chem. Phys. **114**, 10510 (2001).
[12] G. J. A. Sevink, A. V. Zvelindovsky, J. G. E. M. Fraaije, and H. P. Huinink, J. Chem. Phys. **115**, 8226 (2001).
[13] P. Chen, X. He, and H. Liang, J. Chem. Phys. **124**, 104906 (2006).
[14] J. Feng and E. Ruckenstein, Macromolecules **39**, 4899 (2006).
[15] Q. Wang, J. Chem. Phys. **126**, 024903 (2007).
[16] B. Yu, P. Sun, T. Chen, Q. Jin, D. Ding, B. Li, and A.-C. Shi, J. Chem. Phys. **127**, 114906 (2007).
[17] G. J. A. Sevink and A. V. Zvelindovsky, J. Chem. Phys. **128**, 084901 (2008).
[18] A. C. Arsenault, D. A. Rider, N. Tetreault, J. I.-L. Chen, N. Coombs, G. A. Ozin, and I. Manners, J. Am. Chem. Soc. **127**, 9954 (2005).
[19] H. Yabu, T. Higuchi, and M. Shimomura, Adv. Mater. (Weinheim, Ger.) **17**, 2062 (2005).
[20] T. Higuchi, A. Tajima, K. Motoyoshi, H. Yabu, and M. Shimomura, Angew. Chem. **120**, 8164 (2008).
[21] S.-J. Jeon, G.-R. Yi, and S.-M. Yang, Adv. Mater. (Weinheim, Ger.) **20**, 4103 (2008).
[22] T. Tanaka, N. Saito, and M. Okubo, Macromolecules **42**, 7423 (2009).
[23] B. Yu, B. Li, Q. Jin, D. Ding, and A.-C. Shi, Macromolecules **40**, 9133 (2007).
[24] Z.-G. Wang, J. Chem. Phys. **100**, 2298 (1994).
[25] P. D. Olmsted and S. T. Milner, Macromolecules **31**, 4011 (1998).
[26] L. J. Fetters, D. J. Lohse, and W. W. Graessley J. Polym. Sci., Part B: Polym. Phys. **37**, 1023 (1999).